

High-frequency-modulation spectroscopy: phase noise and refractive index fluctuations in optical multipass cells

Peter Werle, MEMBER SPIE

Bernd Jänker

Fraunhofer Institut für Atmosphärische

Umweltforschung

Kreuzeckbahnstrasse 19

82467 Garmisch-Partenkirchen

Germany

E-mail: werle@ifu.fhg.de

Abstract. Substantial improvements of tunable diode laser absorption spectroscopy (TDLAS) with respect to detection speed and limits were obtained by introducing high-frequency modulation schemes, but the expected quantum-limited performance with optical multipass cells has not been attained yet on a routine basis. This paper is primarily devoted to the question of how refractive index fluctuations generated by a turbulent gas flow through an optical multipass cell affect the phase of a frequency-modulated laser beam and therefore influence the performance of highly sensitive spectroscopic measurements. It has been found that for measured pressure fluctuations of about 80 μ bars in such a multipass cell, the expected sensitivity is limited to 7×10^{-7} in terms of optical density, which is more than one order of magnitude above the quantum limit. Further sensitivity improvement by signal averaging is limited by $1/f$ noise contributions from turbulence for integration times longer than 30 s. The consequences of the pressure fluctuations for absorption measurements with tunable diode laser-based systems are discussed with respect to state-of-the-art technology detection limits. © 1996 Society of Photo-Optical Instrumentation Engineers.

Subject terms: multipass cells; refractive index fluctuations; quantum limit; diode laser spectroscopy.

Paper 02085 received Aug. 4, 1995; revised manuscript received Nov. 22, 1995; accepted for publication Nov. 22, 1995.

1 Introduction

In situ trace gas analysis at subparts per billion levels imposes high demands on analytic instrumentation. Fast, accurate, rugged and operational instruments are needed for environmental and process monitoring, medical diagnostics, plasma analysis, and atmospheric research¹⁻⁴. The great number of gaseous pollutants and their generally low variable concentrations with large local differences pose challenging requirements to analytical techniques⁵. Ultra-sensitive instruments free of interference from other atmospheric constituents are required to measure free radicals and other reactive species in the atmosphere. Since the absorption spectrum is characteristic for each molecule, spectroscopic methods allow highly specific detection of many substances. The so-called "fingerprint region" in the mid-infrared from 3 to 20 μ m with strong rotational-vibrational absorption bands is the preferable wavelength region for tunable diode laser absorption spectroscopy (TDLAS), which is being frequently used for measurement of trace gas pollutants in the atmosphere¹⁻⁴.

The TDLAS spectrometers usually work with multipass absorption cells to achieve high sensitivity. To alleviate problems by absorption line overlap, these absorption cells are usually operated at low pressure, where the linewidth has substantial Doppler contribution. In most sensitive instruments, the diode laser is repetitively tuned over an absorption line of a target molecule and the absorption spectra are averaged over a specified time interval. Additional

modulation techniques are used to reduce the $1/f$ -laser noise. With derivative spectroscopy using lock-in detection at kilohertz modulation frequencies, typically detection limits on the order of 0.1 ppbv were achieved for many smaller molecules in the air with spectra averaging times of a few minutes¹⁻⁴. Although these detection limits are sufficient for many applications, still better detection limits are required by modern atmospheric research. Substantial improvements of TDLAS detection speed and detection limits were obtained by using high-frequency modulation (FM) schemes⁶⁻⁹. The FM techniques determine the absorption or dispersion of a narrow spectral feature by detecting the heterodyne beat signal that appears when the frequency-modulated optical spectrum of the probe wave is distorted by the spectral feature of interest. In contrast to conventional derivative spectrometers, where the laser is modulated at several kilohertz, in an FM spectrometer the laser source is modulated with an rf current of about 100 MHz for the so-called single-tone technique^{6,8}. However, to achieve the sensitivity improvement using the FM technique and to build instruments for routine high-sensitivity measurements under field conditions like trace gas flux measurements^{10,11}. Many practical problems still have to be solved.

The absorptions that have to be detected are usually small ($<10^{-5}$), and to achieve sensitivity adequate for environmental monitoring, absorption spectrometers require long optical paths. In instruments with a limited size, long

absorption path lengths up to several hundreds of meters have usually been provided by multireflection optical systems, of which the most well known are the systems invented by White¹² and by Herriott¹³. In all these systems the sensitivity gained by lengthening the absorption path is increasingly offset by the attenuation of the radiation power throughput, due to the increasing number of reflections and the imperfect reflectivity of the mirrors. Consequently, each absorption spectrometer has to be operated with an optimal number of reflections in multireflection absorption systems to achieve the highest signal to noise ratio (SNR). At conditions usually encountered in tunable diode laser spectrometers, the optimal number of passes for the FM spectrometers has been found to be much smaller than the optimal number of passes for the spectrometers using the conventional derivative technique. This finding implies that, if both techniques are operated with an optimal number of passes, the introduction of FM techniques can improve the ultimate SNR in spectrometers using optical multipass cells by only about an order of magnitude. Although still highly desirable, this is substantially lower than the two orders of magnitude potential improvement derived solely from the noise analysis, without considering the use of multipass cells¹⁵.

Trace gas measurements near to the detection limit are usually performed by measuring alternatively the spectrum of the ambient air and the background spectrum, i.e., air devoid of the target substance. This procedure is based on the inherent assumption that within the time interval needed for the acquisition of both spectra the background structures do not move. If this assumption is fulfilled, the subtraction of the background spectrum from the ambient spectrum would provide the absorption spectrum of the target species which, to a first approximation, is only subject to random noise. After the subtraction of background structures, the ambient spectrum is fitted to a calibration spectrum. This spectrum is obtained with the absorption cell filled with calibration gas, which, for example, can be obtained from a permeation-based calibration system. From time to time such a spectrum is recorded and stored for signal processing. Signal processing concepts for TDLAS must provide a means for correcting frequency and amplitude fluctuations as well as having some capability to cope with changing background structures^{16,17}.

Averaging of these filtered spectra should then improve the detection limit according to a square root relationship. This has been tried but the achieved improvement was always substantially smaller than the one expected on the basis of the square root relationship. The observed deviations are most probably caused by the violation of the assumption of stationarity. It is obvious that most systems will have an optimum averaging time determined by the drifts in the system such as temperature changes, moving fringes or background changes. The instrument stability can be described using the Allan variance^{18,19}. As long as white noise dominates the system, the Allan variance is equivalent to the conventional variance and can be used to predict the detection limit of a given system as a function of the integration time¹⁸. A plot of the Allan variance as a function of the integration time usually shows a minimum, which corresponds to the optimum integration time, typically on the order of 40-100 s. This finding has been con-

firmed by many other researchers (private communication from A. Fried, H. Riris, and G. Harris). The optimum integration time is a characteristic property for a given instrument because it reflects the overall stability and therefore can be used to predict the ultimate system performance.

In most sensitive instruments, the diode laser is repetitively tuned over a molecular absorption line and the spectra are averaged over a specified time interval. When the wavelength of the diode laser is tuned over an absorption line, a periodic fringe structure²⁰ is superimposed on the desired signal from the absorption of the target gas ("étalon-effect"). If this fringe structure is generated between the reflecting mirrors in the multipass absorption cell, thermally induced mechanical drifts cause a change of the fringe structure, which usually limits sensitivity due to their variation with time. But even if the losses, which are responsible for the "étalon-effect", could be eliminated, e.g. by an optical isolator, interferometer effects remain and for sensitive measurements, say at optical densities below 10^{-6} , short-term changes in the optical setup of only a few micrometers can significantly influence system performance²¹. Signal fluctuations at low optical densities caused by interferometric effects might provide an explanation for the fact that the expected improvement in system performance after the application of high-frequency modulation schemes to spectroscopic systems designed for conventional derivative spectroscopy has not yet been attained on a routine basis.

The question now is, "What are the short-term fluctuations that limit sensitivity?" As has been mentioned, a limited system stability has been observed by many researchers who use quite different system designs but similar state-of-the-art mechanical, optical, and electronic components with respect to temperature coefficients, for example. While temperature effects seem to dominate when we investigate drift effects, short-term fluctuations might be caused by a turbulent gas flow in the commonly used optical multipass cells.

There are actually three ways in which pressure fluctuations can degrade diode laser performance: The first one relates to the fact that refractive index-induced phase fluctuations affect the measurement in sensitive phase-detection schemes. In this context, pressure fluctuations are shown to cause a change in phase between the carrier and sideband wavelengths. These fluctuations then result in voltage fluctuations out of the phase-sensitive detector, which is set for a constant phase. The second effect relates to the fact that pressure changes in the cell directly result in optical changes. The third effect results from various spatial imaging fluctuations on the detector. In this paper the focus has been on investigations of how fluctuations of the refractive index translate into phase fluctuations of the transmitted laser light and how this effect can be identified as a limiting factor for ultrasensitive FM spectroscopy with multipass cells.

2 Fluctuations of the Refractive index, Optical Path Length and Detection Phase

This paper focuses on problems associated with the propagation of laser beams through turbulent flows in optical multipass cells, where very small changes in the refractive

index are present. These small changes are related primarily to the small local variations in temperature and pressure that are produced by the turbulent motion of the sample gas when the air is expanded from atmospheric pressure into the low-pressure regime of the multipass cell, which is typically operated at a reduced pressure of about 30 mbars. While the refractive index variation from the mean value is very small, in a typical situation of practical interest, a laser beam propagates through a large number of refractive index inhomogeneities, and hence the cumulative effect can be very significant and produce optical phase effects, which in turn lead to angle-of-arrival fluctuations or beam wander, intensity fluctuations, and beam broadening. As an aid in understanding the effects of the refractive index fluctuations, a region of high or low refractive index can be thought of as an eddy, which may behave the same way as a lens. In this model the cell atmosphere may be thought of as a large number of random lenses having different shapes and scale sizes, which move randomly through space. It should be kept in mind, however, that the refractive index is varying within an eddy, and no discontinuities in the refractive index are present. The refractive index of air²² at optical frequencies is given approximately by

$$n = 1 + 77.6 (1 + 7.52 \times 10^{-3} \lambda^{-2}) \times \frac{p}{T} \times 10^{-6}, \quad (1)$$

where p is the atmospheric pressure in millibars, T is the temperature in Kelvin, and λ is the wavelength of light in micrometer. Therefore $(n - 1)$ is a measure of the deviation of the refractive index from its free-space value, and at sea level it has a typical value of 3×10^{-4} . In writing Eq. (1), we have neglected a term that depends, on the water vapor pressure, which contributes significantly less than 1%. A more extensive analysis of optical refractive index can be found in the literature²³⁻²⁵. To estimate detection limits, path length and phase fluctuations, we must know how to relate changes in refractive index to changes in pressure. We accomplish this by finding the differential of (1) and assume a near-infrared spectral region and furthermore do not account for temperature fluctuations, δT , as we were not able to measure the fast fluctuations in our experiments. Then we obtain at room temperature²²

$$\delta n = 78 \times \frac{p}{T} \left(\frac{\delta p}{p} - \frac{\delta T}{T} \right) 10^{-6} \approx 2.6 \times 10^{-7} \delta p (\text{mbar}). \quad (2)$$

The fluctuations in the refractive index translate into fluctuations of the effective optical path length according to

$$\delta L = L_0 \times \delta n, \quad (3)$$

where L_0 is the absorption path length, of a folded laser beam in the optical multipass cell. Typical values range from 10 to 200 m. So far we have a concept to show how pressure fluctuations translate into fluctuations of the optical path length in a multipass cell. Next we will relate this to phase fluctuations in an FM spectrometer.

In a recent publication it has been discussed how a frequency-modulated laser beam can be interpreted as a two-color source, with emission at the laser carrier wave-

Table 1 Effect of small pressure fluctuations, δp , on refractive index, δn , variation in optical path length, δL , and phase jitter, $\delta \phi$, which can ultimately limit the system performance.

Fluctuation of			
Pressure δP	Refractive index δn	Path length δL	Phase $\delta \phi$
30 μbars	7.8×10^{-9}	0.8 μm	2.6×10^{-7}
100 μbars	2.6×10^{-8}	2.6 μm	8.7×10^{-7}
300 μbars	7.8×10^{-8}	7.8 μm	2.6×10^{-6}

length, λ_L , and a sideband, λ_{SB} , obtained by a simultaneous AM-FM modulation of the carrier.²¹ Each of the two beams is related to the absolute absorption path length, L_{abs} , by

$$L_{\text{abs}} = \phi_1 \times \lambda_L \quad (4a)$$

$$L_{\text{abs}} = \phi_2 \times \lambda_{SB}. \quad (4b)$$

Multiplying Eq. (4a) by λ_{SB} and (4b) by λ_L and subsequent subtraction we obtain:

$$L_{\text{abs}} = (\phi_1 - \phi_2) \times \frac{\lambda_{SB} \lambda_L}{\lambda_{SB} - \lambda_L} = \phi \Lambda_s \quad (5)$$

$$\Lambda_s = \frac{\lambda_{SB} \times \lambda_L}{\lambda_{SB} - \lambda_L} = \frac{c}{\nu_{\text{mod}}}, \quad \phi = (\phi_1 - \phi_2),$$

where c is the speed of light in the medium, Λ_s is the beat wavelength, ν_{mod} is the modulation frequency and ϕ is the phase difference between the two beams. This can be rewritten to obtain the relationship between path length fluctuations, δL , and the resulting phase fluctuation, $\delta \phi$,

$$\delta \phi = \delta L / \Lambda_s = \delta L \times \nu_{\text{mod}} / c. \quad (6)$$

These phase fluctuations translate into voltage fluctuations, δU , after applying a phase-sensitive detection scheme (e.g., lock-in technique), which is usually applied in sensitive spectroscopic systems.²⁶ For small changes of the detection phase (i.e., $\sin(\delta \phi) \approx \delta \phi$), we can assume a 1:1 correspondence between phase jitter and phase-sensitive detection voltage jitter²⁷ and thus combining (2), (3), and (6) we measure

$$\delta \phi = \frac{78 \times \nu_{\text{mod}} \times L_0}{c/T} \times 10^{-6} \times \delta p, \quad (7)$$

where again δp is the pressure fluctuation in millibars and T is the temperature in Kelvin. If we apply a frequency modulation scheme to measure weak absorptions and dispersions, we find that these fluctuations of the output voltage are superimposed on the desired signal and therefore degrade the signal-to-noise ratio and system performance. For a modulation frequency ν_{mod} of 100 MHz and an optical pathlength L_0 of 100 m, we can calculate the expected phase fluctuation, $\delta \phi$, from Eq. (7) and we obtain Table 1.

As we can see, pressure fluctuations of about 100 μbars translate into phase fluctuations of about 10^{-6} , which is a

typical value for current detection limits in FM-TDLAS systems applying optical multipass cells. The phase fluctuations have the same statistical properties as refractive index fluctuations and the variations in optical refractive index are caused by variations in pressure and temperature. The refractive index fluctuations that we are considering are those that result from the turbulent flow through a multipass cell and therefore the index of refraction is not a constant, but a function of both time and space.

In practice, we usually expect that signal averaging will improve the detection limits, but care must be taken with appropriate averaging times when determining time averages and we have to ensure stationarity during the averaging interval. The notion of stationarity is the time-domain analogy of spatial homogeneity. Stationarity implies that statistical quantities such as the mean and variance do not vary with time. For example, if we find the mean value at t_0 , it should be identical with the value found at $t_0 + t$. The mean referred to is the ensemble mean or expected value and we average over different realizations of the random process. Unfortunately, we do not have at our disposal an ensemble of identical experimental setups that we may use for simultaneous experiments. Usually we have a single function of time, say, of trace gas concentrations, and we must invoke the assumption of ergodicity to obtain estimates of ensemble averages. An ergodic random process is one in which the infinite time average is equal to its ensemble average and, if we can make this assumption, then we can substitute time averages wherever we have ensemble averages. This leads to another problem. We cannot average forever as required in the ergodic hypothesis. Our only hope is that the process is sufficiently bandlimited so that a reasonable averaging time will give a stable number. How long to average and what filtering effects the averaging time, record length, and sampling rate have on the observations is the subject of an entire area of research-time series analysis.^{27,28} For fluctuations of a stationary random variable ξ , say the index of refraction n or the pressure p , the Wiener-Khinchine theorem establishes a Fourier transform relationship between the autocorrelation function $A(\tau)$, and the power spectrum of a stationary random process, $W_\xi(\omega)$. For $\tau=0$ we obtain the statistical variance from the power spectrum:

$$A_\xi(0) = \int W_\xi(\omega) \times d\omega = \sigma_\xi^2 \equiv \text{variance}. \quad (8)$$

It has been pointed out earlier²⁷ that the mean and variance can be calculated from time series data to obtain a measure of the accuracy and stability. It is assumed that the data are collected over a constant time interval, Δt ; then the time $\tau = k \times \Delta t$ is equivalent to the averaging or integration time. All averages and variances of the $s = 1 \dots m$ subgroups are a function of the integration time τ and the time average of the Allan variance can then be defined as:

$$\langle \sigma_A^2(\tau) \rangle_t = \frac{1}{2m} \times \sum_{s=1}^m [A_{s+1}(\tau) - A_s(\tau)]^2 \quad (9)$$

$$A_s(\tau) = \frac{1}{k} \times \sum_{i=1}^k x_{(s-1)k+i}, \quad s = 1 \dots m \quad \tau = k \times \Delta t.$$

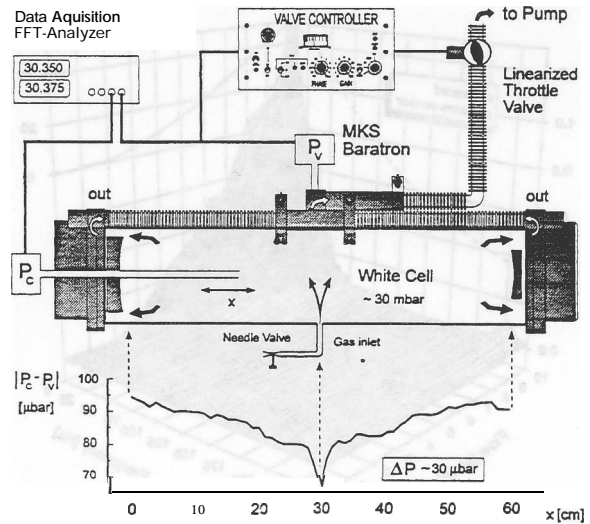


Fig. 1 Experimental setup for the measurement of pressure fluctuations using a calibrated pressure sensor, P_c and a microphone for broadband measurements. The pressure gradient within the optical multipass cell is about $\Delta p = 30 \mu\text{bar}$.

The Allan variance is the time average of the sample variance calculated from adjacent averages $A_k(\tau)$ and $A_{k+1}(\tau)$ of time series data. If we plot $\langle \sigma_A^2(k) \rangle_t$ versus the averaging time τ on a double logarithmic scale, we obtain the Allan plot¹⁸. The noise contributions $S(t)$, which are encountered in most systems, are frequency independent (white) noise and frequency dependent $1/f^\alpha$ ($\alpha \geq 1$) noise, which can be considered as drift. At short integration times τ within a white noise-dominated region, the Allan variance decreases (proportional to $1/\tau$) with increasing integration time. For longer integration times, the Allan variance shifts from this region into a drift-dominated region where it again starts to increase proportional to the measurement time. $1/f$ -type noise contributions will manifest themselves in the Allan plot as a horizontal plateau. It has been mentioned in the previous section that in the white noise dominated region, the square root of the Allan variance is proportional to the detection limit and therefore can be used to predict the detection limit of a given system as a function of the integration time. As we will see in the next section, $1/f$ -type noise contributions, say from turbulence, will limit the signal-to-noise ratio improvement by signal averaging and therefore limit the ultimate sensitivity of a spectrometer.

3 Measurement of Pressure Fluctuations in a White Cell

The experimental setup in Fig. 1 shows a commercial 6 l White cell (Mütek MDS 1600) with a base length of 62.5 cm, which has been used for the investigation of pressure fluctuations caused by a turbulent gas flow. A calibrated pressure sensor (MKS 122 AAX) has been connected to an exhaust valve controller (MKS 252 CX-1) and a linearized throttle valve (MKS 253A) to maintain a constant pressure of about 30 mbars inside the White cell using a 65 m³/h pump (Leybold-Heraeus SV 65). A second pressure sensor (MKS 122 AAX/ 223BD) has been used to record absolute

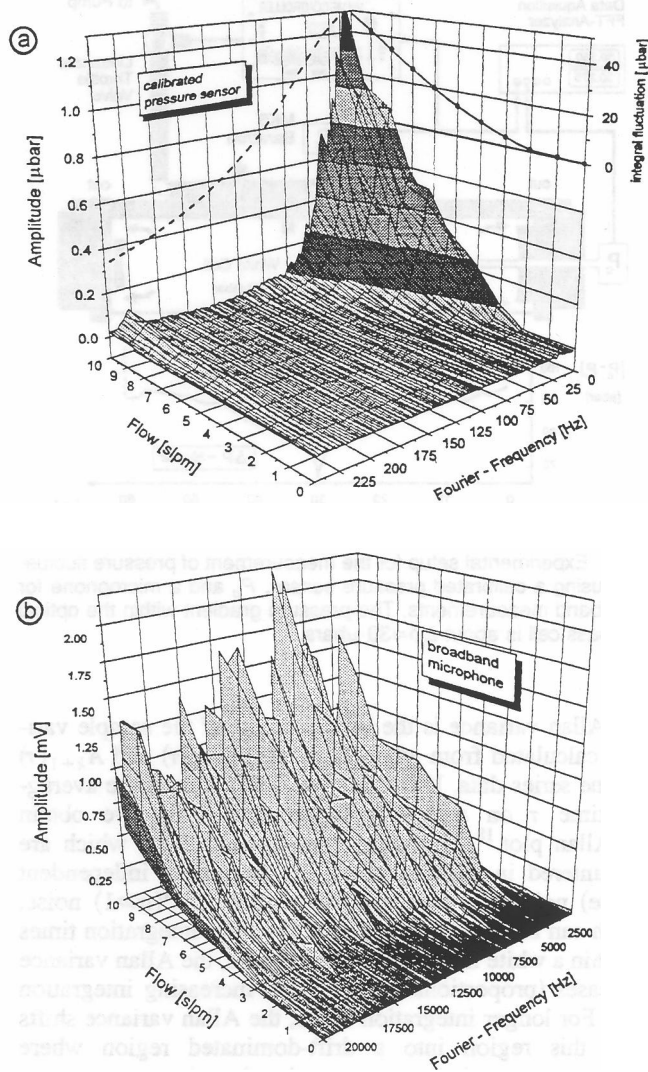


Fig. 2 (a) Low-frequency noise spectra for different air flows of 0..10 liters/min through the cell have been recorded with a calibrated pressure sensor. The integrated fluctuation for a flow of 10 liters/min is $\sigma^2 \sim 50$ pascals and the peak-to-peak variation (-7σ) is in this case also about 50 pascals. The dashed line illustrates the limited bandwidth of the sensor; (b) the same measurement has been repeated with a broadband microphone showing significant contributions at higher Fourier frequencies up to 20 kHz.

pressure as a function of the horizontal displacement x and pressure fluctuations inside the cell with 1 mbar full scale range and $0.1 \mu\text{bar}$ resolution. The sensors have been connected to precision digital multimeters (Prema 6001). In the lower part of Fig. 1 the difference of the two pressure sensors is plotted versus the horizontal displacement x and we observe a pressure drop, ΔP , of $30 \mu\text{bars}$ between the gas inlet ($x=30 \text{ cm}$) and the outlet near the end mirrors ($x=0 \text{ cm}$) of the multipass cell. In order to be able to measure this gradient, the data have been averaged over several measurements.

In the next experiment we used the FFT spectrum analyzer (Advantest R9211 C) to record the frequency distribution of the fast pressure fluctuations at 30 mbars cell pressure and a fixed position x , but now for different gas flows through the cell adjusted manually. Figure 2(a) dis-

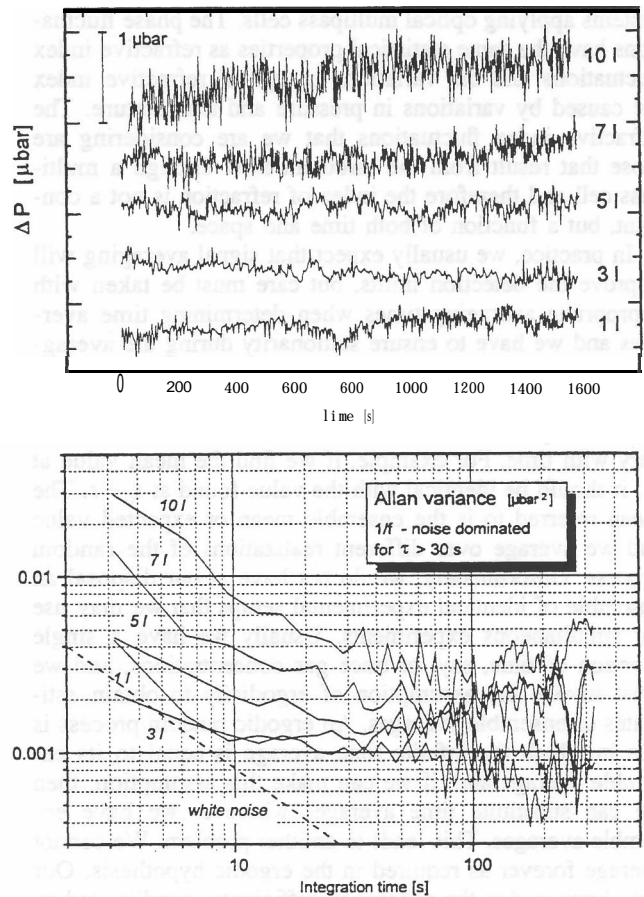


Fig. 3 Time series data from the differential pressure sensor for an air flow 1, 3, 5, 7, and 10 liters/min through the White cell. The corresponding Allan plots show $1/f$ characteristics for integration times τ above 30 s, indicating that further averaging does not reduce the noise.

plays the calibrated amplitude in microbars as a function of Fourier frequencies up to 250 Hz and for flows from 0 to 10 liter/min. It is obvious that an increasing flow corresponds to increasing turbulence and, therefore, we observe increasing pressure fluctuations. According to Eq. (8), the integrated fluctuations have been plotted in the upper right part of Fig. 2(a) as a function of the flow through the multipass cell. A standard deviation of about $7 \mu\text{bars}$ at a flow of 10 liters/min corresponds to a total fluctuation of about $50 \mu\text{bars}$ (7σ), which is superimposed on the gradient displayed in Fig. 1. Unfortunately the calibrated pressure sensor has a limited bandwidth, which is indicated by the dashed line in the upper left part of Fig. 2(a). Therefore, the measurements have been repeated with a high bandwidth microphone and the corresponding Fourier spectra are plotted again versus the flow in Fig. 2(b). Even if these measurements could not be calibrated in pressure units, they show that there is a significant contribution to pressure fluctuations from Fourier frequencies up to at least 20 kHz. Therefore, the total fluctuation displayed in Fig. 2(a) represents only a lower estimate for the fluctuations.

Figure 3 shows some time series data on pressure fluctuations for different flow rates of 1, 3, 5, 7 and 10 liters/min for about 25 min. Again we observe increasing turbu-

lence with increasing flow through the cell. These data have been analyzed in terms of the Allan variance according to Eq. (9) and the results are shown in the lower part of Fig. 3. For short integration times we observe a decrease in the Allan variance proportional to $1/\tau$, as it is expected for white noise. For integration times above 10 s, the spectra become more and more flat and above 30 s they are almost horizontal. The slight increase beyond 100 s at higher flows is due to the drift, which can be observed in the time series data. As the horizontal plateau in the Allan plot indicates a $1/f$ -type noise distribution in the spectral representation, further averaging does not increase sensitivity and therefore turbulent noise represents a dominant limitation.

4 Summary and Discussion of Quantum-Limited Performance

A convenient way to describe the sensitivity at a given signal level is the signal-to-noise ratio. If the noise and not drift effects in the detection system is the limiting factor for ultimate sensitivity, the detection limit of a spectrometer can be derived from the signal-to-noise ratio:

$$SNR = \left[\frac{\langle i_s^2 \rangle}{\langle i_{TN}^2 \rangle + \langle i_{SN}^2 \rangle + \langle i_{1/f}^2 \rangle} \right]^{1/2} \xrightarrow{\text{q.l.}} \sqrt{P_D} \propto \sqrt{N_{Ph}}, \quad (10)$$

where P_D is the laser power impinging upon the detector and N_{Ph} is the corresponding number of photons. The three main noise currents to be considered are the thermal noise (TN) of the detector-preamplifier combination, the quantum (shot) noise (SN) and a $1/f$ -type laser excess noise.¹⁵ While the frequency spectra of thermal noise and quantum noise are generally frequency independent (white noise), the $1/f$ noise contribution is frequency dependent. Wide-band noise measurements indicate that there are regions at modulation frequencies beyond 100 MHz where the $1/f$ noise contribution can be neglected.^{15,21} If we move in detection frequency range into such a potential quantum limited (q.l.) regime, $1/f$ noise contributions can be neglected and the total noise can be approximated as the sum of thermal and shot noise. If sufficient laser power is available on the detector, the power-independent thermal noise does not contribute significantly to the total noise and shot noise remains the dominating contribution. The SNR under such quantum-limited conditions is proportional to the square root of the ratio of the laser power P_D available at the detector. For a typical laser we obtain $N = 3 \times 10^{15}$ photons. According to Poisson statistics, we expect an ultimate lower detection limit of about 2×10^{-8} for quantum-limited conditions.

This fundamental quantum limit is displayed in Fig. 4, where the detection limit in terms of phase jitter is plotted versus the pressure fluctuation in the absorption cell. Superimposed on the "quantum limit" is the phase jitter caused by the refractive index fluctuations, which again are due to pressure changes in the cell. For modulation frequencies of 10 and 100 MHz, the expected relationship between phase and pressure fluctuations for a path length of 100 m is plotted according to Eq. (7). Furthermore, the pressure gradient of about 30 ubars and the lower limit of the peak-to-peak fluctuation of about 50 ubars is displayed. Owing to turbulent refractive index fluctuations, we obtain

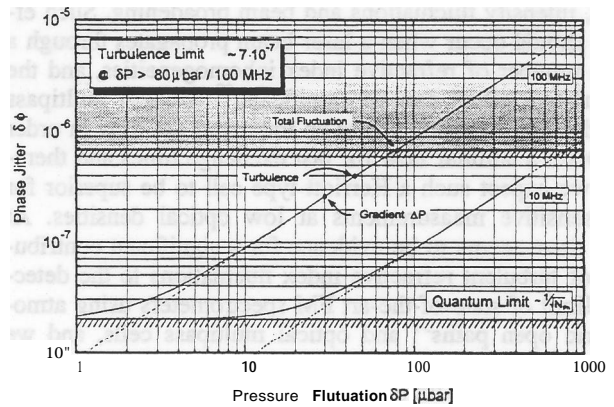


Fig. 4 Phase jitter calculated from the superposition of the pressure gradient and the variations of the index of refraction caused by local pressure fluctuations. The experimental data indicate for the investigated cell a lower limit of about 7×10^{-7} at a flow of 10 liters/min, but significantly higher values can become evident for high-frequency noise contributions.

from the combined effect a limit of 5×10^{-7} in terms of optical density for a modulation frequency of about 100 MHz. The data were derived from measurements at a typical flow of 10 liters/min. For a smaller flow, smaller fluctuations are expected, as we have seen in Figs. 2 and 3. It has also been mentioned that the measured data probably have to be corrected toward higher values, because owing to the limited bandwidth of the calibrated pressure sensor, the contribution of high-frequency fluctuations could not be determined exactly. We estimated from our data a detection limit as indicated by the shaded area in Fig. 4.

One might get the impression from Fig. 4 that the use of lower modulation frequency can improve the situation. Reducing the modulation frequency from 100 MHz to 100 kHz would, if Eq. (6) holds, reduce the phase jitter by three orders of magnitude. To derive the 1:1 correspondence between phase jitter and PSD detection voltage, which we actually measure, we applied the formalism for high-frequency modulation schemes in the limit of the low-frequency modulation index.²¹ The expression for low modulation frequencies and high modulation index with higher order sidebands is more complex and requires the theoretical description of frequency modulation and wavelength modulation spectroscopy? In any case, system operation at lower modulation frequencies, say 100 kHz or even 10 MHz, has to be investigated carefully, because one might run into limitations due to laser excess noise.¹ This is especially important for midinfrared spectrometers using lead-salt diode lasers, where the presence of even spurious side modes substantially increases the laser excess noise, even at 10 MHz. In order to obtain a quantum-limited performance, these excess noise contributions have to be avoided. We have limited the discussion and the formal description in this paper to FM spectrometers, because they have the potential to reach the quantum limit, which has been demonstrated with short absorption cells.^{7,8} However, turbulence effects might also be important for conventional, derivative, or direct absorption spectrometers and we are not aware of any investigation on the effect of turbulence in multipass cells on beam wander, angle-of-arrival fluctua-

tions, intensity fluctuations and beam broadening. Such effects should occur when a laser beam propagates through a large number of refractive index inhomogeneities, and the cumulative effect can be significant.²⁹ Modern multipass cell designs³⁰ already utilize an improved gas flow in order to obtain a laminar flow for fast exchange times and therefore we expect such a Herriott-type cell to be superior for ultrasensitive measurements at low optical densities. At least there seems to be evidence for a significant contribution of turbulent refractive index fluctuations to the detection limit of state-of-the-art FM spectrometers using atmospheric open paths³¹ and optical multipass cells, and we think this effect should be considered for systems designed for near quantum-limited applications.

Acknowledgment

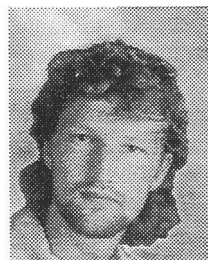
This work was part of work funded by the Bayerisches Staatsministerium für Wirtschaft und Verkehr under contract 3625-VIII/4c. The authors also want to thank Robert Mücke for many stimulating discussions and for proofreading the manuscript. The valuable suggestions of the reviewers are also gratefully acknowledged.

References

- H. I. Schiff, G. I. Mackay, and J. Bechara, "The use of tunable diode laser absorption spectroscopy for atmospheric measurements," *Air Monitoring by Spectroscopic Techniques*, M. W. Sigrist, Ed., Wiley, New York (1994).
- D. J. Brassington, "Tunable diode laser absorption spectroscopy for the measurement of atmospheric species," in *Advances in Spectroscopy*, Vol. 24: Spectroscopy in Environmental Science, R. E. Hester and R. J. Clark, Eds., Wiley, New York (1994).
- R. Grisar, H. Bötter, M. Tacke, and G. Restelli, Eds., *Monitoring of Gaseous Pollutants by Tunable Diode Lasers*, Kluwer Academic Publishers, Dordrecht, Holland (1992).
- H. I. Schiff and U. Platt, Eds., *Optical Methods in Atmospheric Chemistry*, *Proc. SPIE* 1715 (1993).
- L. Newman, *Measurement Challenges in Atmospheric Chemistry*, American Chemical Society, Washington, DC (1993).
- G. C. Bjorklund, "Frequency-modulation spectroscopy: A new method for measuring weak absorptions and dispersions," *Opt. Lett.* **5**, 15-17 (1980).
- C. B. Carlisle, D. E. Cooper, and H. Preier, "Quantum noise-limited FM spectroscopy with a lead-salt diode laser," *Appl. Opt.* **28**, 2567-2576 (1989).
- P. Werle, F. Slemr, M. Gehrtz, and Chr. Bräuchle, "Quantum-limited spectroscopy with a lead-salt diode laser," *Appl. Phys. B* **49**, 99-108 (1989).
- J. M. Supplee, E. A. Whittaker, and W. Lenth "Theoretical description of frequency modulation and wavelength modulation spectroscopy," *Appl. Opt.* **33**, 6294-6302 (1994).
- M. S. Zahniser, D. D. Nelson, J. B. McManus, and P. L. Keabian, "Measurement of trace gas fluxes using tunable diode laser spectroscopy," *Phil. Trans. R. Soc. Lond. A* **351**, 371-382 (1995).
- F. G. Wienhold, H. Frahm, and G. W. Harris, "Measurement of N₂O fluxes from fertilized grassland using a fast response tunable diode laser spectrometer," *J. Geophys. Res.* **99**, 1657-16567 (1994).
- J. U. White, "Very long optical paths in air," *J. Opt. Soc. Am.* **66**, 411-416 (1976).
- D. R. Herriott and H. J. Schulte, "Folded optical delay lines," *Appl. Opt.* **4**, 883-889 (1964).
- P. Werle and F. Slemr, "Signal-to-noise ratio analysis in laser absorption spectrometers using optical multipass cells," *Appl. Opt.* **30**, 430-434 (1991).
- P. Werle, F. Slemr, M. Gehrtz, and Chr. Bräuchle, "Wideband noise characteristics of a lead-salt diode laser: possibility of a quantum noise limited TDLAS performance," *Appl. Opt.* **28**, 1638-1642 (1989).
- H. Riris, C. B. Carlisle, R. E. Warren, and D. E. Cooper, "Signal-to-noise enhancement in frequency modulation spectrometers by digital signal processing," *Opt. Lett.* **19**, 144-146 (1994).
- P. Werle, B. Scheumann, and J. Schandl, "Real time signal processing concepts for trace gas analysis by TDLAS," *Opt. Eng.* **33**, 3093-3105 (1994).
- P. Werle, R. Mücke, and F. Slemr, "The limits of signal averaging in tunable diode laser absorption spectroscopy," *Appl. Phys. B* **57**, 131-139 (1993).
- D. W. Allan, "Statistics of atomic frequency standards," *Proc. IEEE* **54**, 221-230 (1966).
- H. C. Sun and E. A. Whittaker, "Novel étalon fringe rejection technique for laser absorption spectroscopy," *Appl. Opt.* **31**, 4998-5002 (1992).
- P. Werle, "Laser excess noise and interferometric effects in tunable diode laser absorption spectroscopy," *Appl. Phys. B* **60**, 499-506 (1995).
- W. L. Wolfe and G. J. Zisis, Eds., *The Infrared Handbook*, ERIM, Ann Arbor, MI (1989).
- J. C. Owens, "Optical refractive index of air: Dependence on pressure, temperature and composition," *Appl. Opt.* **6**, 51-58 (1967).
- C. A. Friehe, J. C. La Rue, F. H. Champagne, C. H. Gibson, and G. F. Dreyer, "Effects of temperature and humidity fluctuations on the optical refractive index in the marine boundary layer," *J. Opt. Soc. Am.* **65**, 1502-1511 (1975).
- M. L. Wesely and E. C. Alcaraz, "Diurnal cycles of the refractive index structure function coefficient," *J. Geophys. Res.* **78**, 6224 (1973).
- P. Werle, "Spectroscopic trace gas analysis using semiconductor diode lasers," *Spectrochim. Acta* **A52(8)** 805-822 (1996).
- G. M. Jenkins and D. G. Watts, *Spectral Analysis and its Applications*, Holden-Day, San Francisco (1968).
- N. Wiener, *Extrapolation, Interpolation and Smoothing of Stationary Time Series*, Wiley, New York (1949).
- J. W. Strohbehn, Ed., *Laser Beam Propagation in the Atmosphere*, Springer-Verlag, New York (1978).
- J. B. McManus, P. L. Keabian, and M. S. Zahniser, "Astigmatic mirror multipass absorption cells for long-path-length spectroscopy," *Appl. Opt.* **34**, 3336-3348 (1995).
- H. Riris, C. B. Carlisle, L. W. Carr, D. E. Cooper, R. U. Martinelli, and R. J. Menna, "Design of an open path near-infrared diode laser sensor: Application to oxygen, water, and carbon dioxide vapor detection," *Appl. Opt.* **33**, 7059-7066 (1994).



Peter Werle works as a section manager at the Fraunhofer Institute for Atmospheric Environmental Research in Garmisch-Partenkirchen, where he is responsible for the development of integrated systems for trace gas analysis. He received the Diplom-Physiker degree from the University of Mainz, and his Dr. rer. nat degree from the University of Munich in 1989. His current research interests focus on improving the sensitivity and detection speed of spectroscopic instrumentation for trace gas analysis, ultrasensitive FM spectroscopy using semiconductor diode lasers, digital signal processing and interferometric measurement techniques. Dr. Werle is a member of the Deutsche Physikalische Gesellschaft, the Optical Society of America, and SPIE.



Bernd Jänker received his Diplom Ingenieur degree in mechanical engineering from the Fachhochschule München Germany. He works at the Fraunhofer Institute for Atmospheric Environmental Research in Garmisch-Partenkirchen on calibration, systems and the mechanical and optical engineering of components and sub-systems for tunable diode laser spectrometers.